

# Intestinal receptor of SARS-CoV-2 in inflamed IBD tissue is downregulated by HNF4A in ileum and upregulated by interferon regulating factors in colon

Bram Verstockt, MD PhD<sup>1,2#</sup>; Sare Verstockt, MSc PhD<sup>2#</sup>; Saeed Abdu Rahiman, MSc<sup>2</sup>; Bo-jun Ke, MSc<sup>2</sup>; Kaline Arnauts, MSc<sup>2,3</sup>; Isabelle Cleynen, MSc PhD<sup>4</sup>; João Sabino, MD PhD<sup>1,2</sup>; Marc Ferrante, MD PhD<sup>1,2</sup>; Gianluca Matteoli, DVM PhD<sup>2\$</sup>; Séverine Vermeire, MD PhD<sup>1,2\$\*</sup>

# contributed equally

\$ contributed equally

<sup>1</sup> Department of Gastroenterology and Hepatology, University Hospitals Leuven, KU Leuven, Leuven, Belgium

<sup>2</sup> Department of Chronic Diseases, Metabolism and Ageing (CHROMETA), Translational Research Center for Gastrointestinal Disorders (TARGID), KU Leuven, Leuven, Belgium

<sup>3</sup> Department of Development and Regeneration, Stem Cell Institute Leuven (SCIL), KU Leuven, Leuven, Belgium

<sup>4</sup> Department of Human Genetics, Laboratory for Complex Genetics, KU Leuven, Leuven, Belgium

## Corresponding author

Séverine Vermeire, MD, PhD

Department of Gastroenterology and Hepatology, University Hospitals Leuven

Herestraat 49 3000 Leuven, Belgium.

Phone: 0032 (0)16 34 42 18

@ibdleuven @TARGID\_KULEUVEN @bverstockt @SareVerstockt @gmatteoli1978 @JoaoPGSabino

@ICleynen @saeedfc

E-mail: [severine.vermeire@uzleuven.be](mailto:severine.vermeire@uzleuven.be)

**Total word count:** 4343

**Total number of figures / tables:** 7 / 0

**Total number of references:** 62

## 1 **ABBREVIATIONS**

|    |          |  |
|----|----------|--|
| 2  | ACE      | angiotensin converting enzyme                |
| 3  | adj      | adjusted                                     |
| 4  | COVID-19 | coronavirus disease 2019                     |
| 5  | CD       | Crohn's disease                              |
| 6  | CRC      | colorectal cancer                            |
| 7  | DPP4     | dipeptidyl peptidase 4                       |
| 8  | FC       | fold change                                  |
| 9  | FDR      | false discovery rate                         |
| 10 | HNF4A    | hepatocyte nuclear factor 4 Alpha            |
| 11 | GEM      | gel beads in emulsion                        |
| 12 | IBD      | inflammatory bowel disease                   |
| 13 | IFN      | interferon                                   |
| 14 | IL       | interleukin                                  |
| 15 | IPA      | ingenuity pathway analysis                   |
| 16 | IQR      | interquartile range                          |
| 17 | MAF      | minor allele frequency                       |
| 18 | MERS     | middle east respiratory syndrome             |
| 19 | RAS      | renin-angiotensinogen system                 |
| 20 | RNA      | ribonucleic acid                             |
| 21 | SARS     | severe acute respiratory syndrome            |
| 22 | SCENIC   | Single Cell Network Inference                |
| 23 | TMPRSS   | transmembrane protease serine                |
| 24 | TNF      | tumour necrosis factor                       |
| 25 | UC       | ulcerative colitis                           |
| 26 | WGCNA    | weighted gene co-expression network analysis |
| 27 |          |  |

## 28 **ABSTRACT**

29 Patients with IBD are considered immunosuppressed, but do not seem more vulnerable for COVID-19.  
30 Nevertheless, intestinal inflammation has shown an important risk factor for SARS-CoV-2 infection and  
31 prognosis. Therefore, we investigated the effect of intestinal inflammation on the viral intestinal entry  
32 mechanisms, including *ACE2*, in IBD.

33 We collected (un)inflamed mucosal biopsies from CD (n=193) and UC (n=158) patients, and 51 matched  
34 non-IBD controls for RNA sequencing, differential gene expression and co-expression analysis. Organoids  
35 from UC patients were subjected to an inflammatory mix and processed for RNA sequencing. Transmural  
36 ileal biopsies were processed for single-cell (sc) sequencing. Publicly available colonic sc-RNA sequencing  
37 data, and microarrays from tissue pre/post anti-TNF therapy, were analyzed.

38 In inflamed CD ileum, *ACE2* was significantly decreased compared to control ileum ( $p=4.6E-07$ ), whereas  
39 colonic *ACE2* expression was higher in inflamed colon of CD/UC compared to control ( $p=8.3E-03$ ;  $p=1.9E-$   
40  $03$ ). Sc-RNA sequencing confirmed this *ACE2* dysregulation, and exclusive epithelial *ACE2* expression.  
41 Network analyses highlighted *HNF4A* as key regulator of ileal *ACE2*, while pro-inflammatory cytokines and  
42 interferon regulating factors regulated colonic *ACE2*. Inflammatory stimuli upregulated *ACE2* in UC  
43 organoids ( $p=1.7E-02$ ), not in non-IBD controls ( $p=9.1E-01$ ). Anti-TNF therapy restored colonic *ACE2*  
44 dysregulation in responders.

45 Intestinal inflammation alters SARS-CoV-2 coreceptors in the intestine, with opposing effects in ileum and  
46 colon. *HNF4A*, an IBD susceptibility gene, is an important upstream regulator of *ACE2* in ileum, whereas  
47 interferon signaling dominates in colon. Our data support the importance of adequate control of IBD in order  
48 to reduce risk of (complicated) COVID-19.

49  
50 **Keywords:** COVID-19; *ACE2*; *TMPRSS2*; inflammatory bowel diseases; SARS-CoV-2; *HNF4A*;  
51 interferon; organoids; transcriptomics; single cell; intestinal inflammation

52

## 53 INTRODUCTION

54 Since the novel betacoronavirus SARS-CoV-2 was first reported in the province of Wuhan, China, at the  
55 end of 2019, the virus has spread over more than 200 countries, causing more than 8.9 million infections,  
56 including almost 470,000 death globally.<sup>1</sup> Despite being primarily a respiratory virus, coronavirus disease  
57 2019 (COVID-19) can also present with non-respiratory signs, including digestive symptoms as diarrhea,  
58 nausea and ageusia.<sup>2, 3, 4</sup>

59  
60 Although it is thought that SARS-CoV-2 primarily infects the lungs with transmission via the respiratory  
61 route, the gastro-intestinal tract can be an alternative viral target organ. Indeed, the SARS-CoV-2 receptor  
62 angiotensin converting enzyme 2 (ACE2) is highly expressed on differentiated enterocytes, with strong  
63 induction of generic viral response programs upon viral binding.<sup>5, 6</sup> The cellular entry of coronaviruses  
64 depends on the binding of the spike (S) protein to a specific receptor, followed by an S protein priming by  
65 proteases, with key players ACE2 (receptor for the S protein) and TMPRSS2 (protease) in case of COVID-  
66 19.<sup>6, 7, 8</sup> Furthermore, based on protein crystal structures, data predicted that the Middle East respiratory  
67 syndrome (MERS)-CoV receptor dipeptidyl peptidase 4 (DDP4) might act as a candidate binding target or  
68 co-receptor of SARS-CoV-2.<sup>9, 10</sup> In line, proteomic studies in COVID-19 patients suggested a prognostic  
69 role for DDP4.<sup>11</sup> Upon cellular entry in nasal goblet secretory cells, lung type II pneumocytes and ileal  
70 absorptive enterocytes, an interferon-driven mechanism is initiated, including the upregulation of *ACE2*  
71 which further enhances infection.<sup>7</sup>

72  
73 Why *ACE2*, the S protein receptor, is abundantly expressed on intestinal epithelium, is not entirely  
74 understood. Recent studies have addressed the homeostatic role of ACE2 on intestinal epithelial cells  
75 demonstrating defective intestinal amino acid absorption in ACE2 deficient mice.<sup>12</sup> Mechanistically, ACE2  
76 independently of its role on the renin angiotensin system (RAS), is essential for regulating epithelial  
77 tryptophan absorption, expression of antimicrobial peptides, and consequently regulating the ecology of the  
78 gut microbiome promoting homeostasis and preventing intestinal inflammation.<sup>13</sup> Thus, ACE2 regulation  
79 could be link to the pathogenesis of IBD, playing a role as modulator of epithelial immune homeostatic  
80 functions.

81

82  
83 Individual susceptibility to COVID-19 may correlate with the expression of these designated (co)receptors.  
84 In this respect, it is unknown how inflammation affects *ACE2*, *TMPRSS2* and/or *DDP4* expression in ileum  
85 and colon. Inflammatory Bowel Disease (IBD) is a prototype gastrointestinal disease characterized by a  
86 chronic relapsing inflammatory infiltrate of the small and/or large bowel. So far, data on COVID-19 in  
87 patients with IBD are rather limited,<sup>14, 15, 16, 17, 18</sup> although suggest that increasing age, a diagnosis of  
88 ulcerative colitis [UC] (as opposed to Crohn's disease [CD]) and increasing disease activity are linked with  
89 a more severe course of COVID-19. In contrast, anti-inflammatory IBD therapy has not yet been associated  
90 with COVID-19 risk. Using a combination of bulk and single cell transcriptomics and organoid cultures, we  
91 studied the intestinal expression of several SARS-CoV-2 co-receptors in the healthy gut and in IBD and  
92 investigated whether inflammation alters co-receptor expression.

93

## 94 **MATERIALS AND METHODS**

### 95 **Patients**

96 This study was carried out at the University Hospitals Leuven (Leuven, Belgium). All included patients had  
97 given written consent to participate in the Institutional Review Board approved IBD Biobank of University  
98 Hospitals Leuven, Belgium (B322201213950/S53684 and B322201110724/S52544). Endoscopy-derived  
99 (un)inflamed mucosal biopsies were obtained cross-sectionally from IBD patients requiring colonoscopy  
100 during routine care (**Supplementary Table S1**). Samples from individuals undergoing colonoscopy for  
101 polyp detection were included as controls. Transmural ileal biopsies, derived during right hemicolectomy  
102 from CD patients and patients with colorectal cancer (CRC), were collected, stored in RPMI-1640 medium  
103 on ice until single cell isolation.

104

### 105 **Organoids**

106 Mucosal biopsies from both uninflamed and macroscopically inflamed colon segments (UC only) were  
107 processed as reported earlier.<sup>19</sup> In brief, crypts were isolated and cultured as organoids for at least four  
108 weeks. Inflammation was then re-induced using an inflammatory mix (100 ng/ml TNF- $\alpha$ , 20 ng/ml IL-1 $\beta$ ,  
109 1 $\mu$ g/ml Flagellin) during 24 hours.<sup>19</sup>

## 110 **Bulk transcriptomics**

111 Inflamed biopsies were taken at the most affected site at the edge of an ulcerative surface, whereas  
112 uninfamed biopsies were taken randomly in macroscopic unaffected areas. All were stored in RNALater  
113 buffer (Ambion, Austin, TX, USA) and preserved at -80°C. As described previously,<sup>20</sup> RNA from biopsies  
114 was isolated using the AllPrep DNA/RNA Mini kit (Qiagen, Hilden, Germany), and RNA libraries were  
115 prepared using the TruSeq Stranded mRNA protocol (Illumina, San Diego, USA). RNA from organoids was  
116 extracted using the RNeasy Mini Kit (Qiagen) and libraries were constructed by the Lexogen QuantSeq 3'  
117 mRNA-Seq Library Kit FWD (Lexogen, Vienna, Austria).<sup>19</sup> All RNA libraries were sequenced by the Illumina  
118 HiSeq4000 (Illumina, San Diego, CA). Raw sequencing data were aligned to the reference genome  
119 (GRCh37) using Hisat2 (version 2.1.0)<sup>21</sup> and absolute counts generated using HTSeq.<sup>22</sup> Counts were  
120 normalized and protein coding genes selected (Ensemble hg 19 reference build)<sup>23</sup> using the DESeq2  
121 package.<sup>24</sup> A weighted gene co-expression network (WGCNA) was generated,<sup>25</sup> as described earlier.<sup>26, 27</sup>  
122 The module eigengene was defined as the first principal component summarizing the expression patterns  
123 of all genes into a single expression profile within a given module. Genes showing the highest correlation  
124 with the module eigengene were referred to as hub genes. Pathway and upstream regulator analyses were  
125 performed using Ingenuity Pathway Analysis (IPA, QIAGEN, Aarhus, Denmark), with network visualization  
126 via Cytoscape (v3.8.0).<sup>28</sup> Publicly available microarray datasets of ileal and colonic biopsies (GEO  
127 GSE14580, GSE12251, GSE16879) were accessed to investigate the effect of anti-TNF therapy on genes  
128 of interest.<sup>29, 30</sup>

129

## 130 **Single cell transcriptomics**

131 Transmural ileal samples were treated with 1mM DTT and 1mM EDTA in 1x Hank's balanced salt solution  
132 (HBSS), and 1mM EDTA in HBSS at 37°C for 30 minutes, respectively. Then, tissue was transferred into a  
133 sterile gentleMACS C tube (Miltenyi Biotec), and digested with 5.4 U/mL collagenase D (Roche applied  
134 science), 100 U/mL DNase I (Sigma) and 39.6 U/mL dispase II (Gibco) with the gentleMACS™ Dissociator  
135 (program human\_tumor\_02.01). Samples were incubated for 30 minutes at 37°C at 250 rpm. Dissociated  
136 samples were filtered with 70 µm cell strainers, and treated with red blood cell lysis buffer (11814389001,  
137 Roche). After centrifugation, single-cell suspensions were re-suspended in 0.4% BSA in PBS, and were  
138 immediately processed with 10x 3' v3 GEM kit, and loaded on a 10x chromium controller to create Single

139 Cell Gel beads in Emulsion (GEM). A cDNA library was created and assessed using a 10x 3' v3 library kit,  
140 and was then sequenced on a NovaSeq 6000 system (Illumina). Pre-processing of the samples including  
141 alignment, and counting was performed using Cell Ranger Software from 10x (Version: 3.0.2).

142  
143 Publicly available colonic single cell RNA sequencing data (sc-RNA seq) (Single Cell Portal, SCP 259)  
144 were downloaded and visualized using the SCP data browser.<sup>31</sup> For colonic epithelial single cell data, tSNE  
145 coordinates and publicly available annotation with the data was used for visualization and analysis.

146  
147 Annotation of the ileal data was performed using SingleR R package, with inbuilt Human Cell Atlas data as  
148 reference. Quality control, clustering and dimensionality reduction of sc-RNA seq data was performed using  
149 Seurat R package (Version 3.1.5).<sup>32, 33</sup> Data from each 10x run were integrated after performing  
150 SCTransform on each dataset, with percentage of mitochondrial genes set as a parameter to be regressed.  
151 Single Cell Network Inference (SCENIC) analysis was performed using a python implementation of the  
152 SCENIC pipeline (PySCENIC) (Version 0.9.19).<sup>34</sup>

153

#### 154 **Immunofluorescence staining**

155 Transmural ileal biopsies, obtained during abdominal surgery in patients with IBD and CRC, were fixed in  
156 4% formalin, embedded in paraffin and sections of 5µm were cut (Translational Cell & Tissue Research  
157 Laboratory, University Hospitals Leuven and at VIB & KU Leuven Center for Brain & Disease Research).  
158 After deparaffinization, antigen retrieval was done in Tris-EDTA buffer (10 mM Tris base, 1 mM EDTA  
159 solution, 0.05% Tween 20, pH 9.0) at 95°C for 30 minutes. 1% BSA in PBST (0.1% tween-20 and 0.5%  
160 sodium azide) was used to block non-specific binding of detection antibodies and gently permeabilize  
161 before ACE2 and Cytokeratin AE1/AE3 staining. In brief, ACE2 (Polyclonal, Cell Signaling Technology) and  
162 cytokeratin (IgG1-kappa, clone AE1/AE3, Dako) were applied in 1% BSA, followed by donkey anti-rabbit  
163 Cy3 (Jackson Immuno Research) and donkey anti-mouse Alexa fluor 488 (Invitrogen). Slides were mounted  
164 in SlowFade™ Diamond Antifade Mountant (Invitrogen), and stored at 4 °C before imaging. Images were  
165 acquired using a Zeiss LSM 780 at the Cell and Tissue Imaging Cluster (CIC) at KU Leuven.

166

## 167 **Genetics**

168 All samples were genotyped using the Illumina GSA array. All SNPs and samples with more than 10%  
169 missingness rate were removed, as were SNPs with minor allele frequency (MAF)<0.001. Genotypes for  
170 rs6017342 (*HNF4A*) were extracted. All steps were performed using PLINK (v1.90b4.9).<sup>35</sup>

171

## 172 **Statistical analysis**

173 Statistical analysis was performed using R 3.6.2 (The R foundation, Vienna, Austria). Pearson correlation  
174 coefficients were computed to assess the correlation between individual genes. Multivariate analysis was  
175 performed using the R package “lm.beta”. Continuous variables on graphs were expressed as median and  
176 interquartile range (IQR). *ACE2*, *DPP4* and *TMPRSS2* comparisons were done using two sample t-tests or  
177 Wilcoxon tests, as appropriate. In case of hypothesis-free comparisons, ie. genome-wide differential gene  
178 expression analyses, multiple testing correction was applied (adjusted p [adj. p], Benjamini-Hochberg  
179 method).

180

## 181 **RESULTS**

### 182 **Intestinal *ACE2*, *TMPRSS2* and *DPP4* expression in IBD patients versus non-IBD controls**

183 First, we studied the expression patterns of *ACE2*, *DPP4* and *TMPRSS2* in ileum and colon biopsies from  
184 351 IBD patients (193 CD, 158 UC) and 51 non-IBD controls based on bulk RNA sequencing.

185

186 In non-IBD controls, *ACE2* and *DPP4* expression levels were strongly increased in ileum compared to colon  
187 (fold change (FC) =32.0, p=6.3E-13; FC=16.5, p=6.3E-13) (**Figure 1A-B**). In contrast, ileal *TMPRSS2* was  
188 lower compared to colon (FC=-2.9, p=6.3E-13) (**Figure 1C**).

189

190 When turning to tissue from IBD patients, *ACE2* and *DPP4* levels in uninfamed IBD ileum were similar to  
191 those observed in matched control ileum (p=1.6E-01; p=8.0E-01) (**Figure 1A-B**). *TMPRSS2* however, was  
192 significantly upregulated compared to control ileum (FC=1.2, p=3.4E-02) (**Figure 1C**). In uninfamed IBD



193 colon, expression levels of *ACE2*, *DDP4* and *TMPRSS2* did not differ from control colon ( $p=2.0E-01$ ;  
194  $p=3.3E-01$ ;  $2.2E-01$ ) (**Figure 1A-C**).

195  
196 In inflamed CD ileum, *ACE2* and *DPP4* expression was significantly decreased compared to control ileum  
197 ( $FC=-2.8$ ,  $p=4.4E-07$ ;  $FC=-2.5$ ,  $p=1.4E-06$ ) (**Figure 1A-B**). *TMPRSS2* behaved opposite, with a significant  
198 upregulation in inflamed ileum versus control ileum ( $FC=1.4$ ,  $p=1.8E-03$ ) (**Figure 1C**). At colonic level,  
199 *ACE2* expression was higher in inflamed CD and UC colon than in control colon ( $FC=1.4$ ,  $p=2.5E-02$ ;  
200  $FC=1.4$ ,  $p=2.0E-02$  respectively) (**Figure 1A**). Except for a decrease in *DPP4* expression in inflamed CD  
201 colon versus control colon ( $FC=1.3$ ,  $p=4.6E-02$ ), no dysregulations were observed for colonic *DPP4* and  
202 *TMPRSS2* ( $p=1.8E-01$ ;  $p\leq 3.4E-01$ ) (**Figure 1B-C**).

203  
204 Despite *ACE2* being X-linked, multivariate analysis did not reveal any contribution of sex to mucosal *ACE2*  
205 expression ( $p=5.1E-01$ ), nor of age ( $p=1.4E-01$ ), diagnosis ( $p=5.6E-01$ ) or disease duration ( $p=5.2E-01$ ).  
206 Intestinal *ACE2* expression was significantly affected by biopsy location ( $p=2.8E-34$ ) and inflammatory state  
207 ( $p=4.2E-12$ ).

208

### 209 **Gene co-expression analysis of the *ACE2*-, *DPP4*- and *TMPRSS2*-related networks**

210 To get a better understanding of the biological network of *ACE2*, *DPP4* and *TMPRSS2*, we performed  
211 WGCNA on all mucosal biopsies.

212

213 At ileal level, we identified 18 co-expression modules (clusters) ranging in size from 106 to 1465 genes  
214 (**Figure 2A**). One module contained both *ACE2* and *DPP4* (module “blue”; 1134 genes) (**Supplementary**  
215 **Table S2**). The strongest correlation with the eigengene (i.e. the principal component) of this *ACE2/DPP4*-  
216 module was found for hub genes *MMP5* ( $r=0.94$ ,  $p=8.6E-74$ ), *ZNF664* ( $r=0.94$ ,  $p=3.7E-71$ ) and *DPP4*  
217 ( $r=0.93$ ,  $p=1.2E-68$ ) (**Figure 2A**). Moreover, *ACE2* also seemed to have a central role in this co-expression  
218 network with a correlation value of  $r=0.86$  ( $p=4.6E-45$ ) (**Figure 2A**). Pathway analysis of the *ACE2/DPP4*-  
219 module found enrichment for epithelium-related metabolic pathways such as Xenobiotic Metabolism  
220 Signaling, Nicotine Degradation II and Melatonin Degradation ( $p<1.0E-08$ ). Predicted upstream analysis

221 (using curated datasets in IPA) highlighted the transcription regulator HNF4A, an IBD susceptibility gene,  
222 as the most likely upstream regulator of the *ACE2/DPP4*-module ( $p=1.2E-11$ ).  
223 *TMPRSS2* belonged to a separate module “yellow” (1126 genes) with hub gene *COA3* ( $r=0.92$ ,  $p=4.7E-61$ )  
224 (**Figure 2A, Supplementary Table S3**). Genes within this module were mainly related to mitochondrial  
225 functions (eg. Oxidative Phosphorylation, Mitochondrial dysfunction and Sirtuin Signaling,  $p<1.6E-29$ ), and  
226 their top upstream regulator was again HNF4A ( $p=1.5E-27$ ).

227  
228 At colonic level, 24 co-expression modules were present ranging in size from 128 to 2267 genes (**Figure**  
229 **2B**). In contrast to the ileum, colonic *ACE2* and *DPP4* were not co-expressed (**Supplementary Tables S3**),  
230 with *ACE2* being part of module “green” (797 genes). Here, *ACE2* co-clustered with *TMPRSS2*. The *ACE2*-  
231 module with top hub gene *TMEM63B* ( $r=0.89$ ,  $p=5.8E-81$ ) did not show significant enrichment for specific  
232 pathways. Upstream analysis of this module ranked TNF and again HNF4A as the top regulators ( $p=7.7E-$   
233  $06$ ;  $p=9.4E-03$ ).

234  
235 Lastly, we studied the relationship between mucosal *ACE2* and *HNF4A* expression levels. Ileal *ACE2*  
236 expression strongly correlated with ileal *HNF4A* expression ( $r=0.69$ ,  $p<2.2E-16$ ), whereas colonic levels  
237 showed limited correlation ( $r=0.2$ ,  $p=1.3E-03$ ) (**Supplementary Figure S1**).

238  
239 **Single nucleotide polymorphisms in *HNF4A* linked to *ACE2* expression in ileum but not in**  
240 **colon**

241 As the expression of *ACE2*-modules was found to be driven by the IBD susceptibility locus, *HNF4A*, we  
242 next studied the genetic variability in rs6017342 (i.e. the causal IBD variant in this locus, <sup>36</sup>), and its  
243 relationship with *ACE2* and *HNF4A* expression, both in inflamed ileum and colon. Ileal *ACE2* levels were  
244 lower in patients carrying the *HNF4A*-AA genotype, compared to patients carrying the C-allele, i.e. *HNF4A*-  
245 AC or *HNF4A*-CC genotypes ( $p=2.8E-02$ ) (**Figure 3**). Colonic *ACE2* expression was independent of the  
246 *HNF4A* genotype ( $p=6.7E-01$ ).

247  
248

249 **Decrease of ACE2/TMPRSS2 double positive cells in inflamed ileum, but not in colon**

250 *ACE2* expression in the gastrointestinal tract is primarily found in absorptive enterocytes,<sup>7, 37</sup> which could  
251 indirectly be confirmed through the significant correlation ( $p < 2.2E-16$ ) between mucosal *ACE2* and several  
252 epithelial marker genes (*APOA1*, *SI*, *FABP6*, *ENPEP*) (**Supplementary Figure S2**). To further examine  
253 the expression of genes associated with risk of SARS-CoV-2 infection in IBD patients, we employed sc-  
254 RNA seq to profile transmural biopsies of (un)inflamed regions of resected tissue from six CD patients  
255 undergoing ileocaecal resection. Unaffected ileal tissue from five patients with CRC undergoing right  
256 hemicolectomy was used as control. A total of 78,722 cells were used for downstream analyses containing  
257 a similar number of cells from each type of tissue (inflamed CD, uninfamed CD and healthy tissue)  
258 (**Supplementary Figure S3B**). Sixty-one cell clusters belonging to epithelial, immune and stromal cells  
259 were obtained using unsupervised clustering (**Figure 4A, Supplementary Figure S3A**). Cell clusters were  
260 annotated by correlating the cluster gene expression profiles with Human Cell Atlas using SingleR, as  
261 previously described.<sup>38</sup> *ACE2* expression was found exclusively in epithelial cell clusters (**Figure 4B-C**),  
262 which could also be confirmed using immunofluorescence staining (**Figure 5**). To define the epithelial cell  
263 subtypes expressing *ACE2* at deeper resolution, clusters annotated as epithelial cells by SingleR were  
264 extracted and re-clustered (**Figure 4D**). The re-clustered epithelial cell subtypes were annotated using a  
265 marker panel designed based on previous reports (**Supplementary Figure S3C**).<sup>39</sup> Three enterocyte  
266 clusters were identified, out of which two clusters co-expressed *ACE2*, *TMPRSS2* and *DPP4*. Most  
267 prominent *ACE2* expression was observed in the ACE2/TMPRSS2 Enterocytes 1 cluster (**Figure 4G-I**,  
268 **Supplementary Figure S3D**).

269  
270 Next, we asked whether *ACE2* expression varied across ileal tissue with inflammatory state, as observed  
271 in our bulk transcriptomic data (**Figure 1A**). *ACE2* expression and frequency of *ACE2* positive cells were  
272 clearly reduced in ileum of patients with active CD, compared to uninfamed or healthy tissue (**Figure 4E-**  
273 **F, Supplementary Figure S3E**). A similar reduction of *DPP4* expression was observed in the inflamed  
274 samples in the ACE2/TMPRSS2 Enterocytes 1 and ACE2/TMPRSS2 Enterocytes 2 clusters (**Figure 4E**).  
275 In line, reduction of *ACE2* expression in inflamed ileum compared to healthy tissue was also confirmed with  
276 confocal imaging (**Figure 5**).

277

278 To define *ACE2* expression in healthy and inflamed colon, we visualized publicly available colonic sc-RNA  
279 seq data containing 366,650 cells from colonic mucosa obtained in 18 (in)active UC patients and 12 healthy  
280 individuals (Single Cell Portal, SCP 259) (**Supplementary Figure S4A-C**).<sup>31</sup> As for the ileum, *ACE2* was  
281 solely expressed in colonic epithelium, mainly in a subset of enterocyte (**Figure 6A-B, Supplementary**  
282 **Figure S4D**). As in the ileum, the *ACE2* positive colonic enterocyte cluster co-expressed *TMPRSS2* and  
283 *DPP4* (**Figure 6B, 6E-G**). However, in contrast to ileum, colonic *ACE2* expression was mainly restricted to  
284 enterocytes isolated from patient with active UC, while undetectable in colonic enterocytes isolated from  
285 the mucosa of healthy subjects. (**Figure 6C-D, Supplementary Figure S4E**)

286  
287  
288 To compare expression and regulation of *ACE2* between colon and ileum, we performed an integrated  
289 analysis of epithelial cells from colon and ileum (**Supplementary Figure S5A-B**). In colonic *ACE2* positive  
290 epithelial cells, *ACE2* expression was lower compared levels in ileal *ACE2* positive epithelial cells (**Figure**  
291 **6H**). Furthermore, using SCENIC we performed genomic regulatory networks analysis of the epithelial cells  
292 to identify specific transcription programs in *ACE2* expressing enterocytes, both in ileum and colon. As  
293 demonstrated using bulk RNA analysis, we found a relatively higher *HNF4A* regulon activation in ileal *ACE2*  
294 positive cells, compared to colonic *ACE2* enterocytes (**Figure 6I**). Differently, colonic *ACE2* expressing  
295 enterocytes were found to have increased regulon activity of interferon responsive factors, such as IRF6  
296 and IRF7, when compared to ileum (**Figure 6I**).

297  
298  
299 **Ileum and colon: different key regulators in *ACE2* positive cells**

300 We then asked whether particular expression patterns within *ACE2* positive cells depend on the tissue  
301 and/or inflammatory state, and studied which upstream regulators were linked to these changes. When  
302 comparing expression profiles of *ACE2* positive cells from inflamed CD ileum with control ileum, we found  
303 56 differentially expressed genes (adj.  $p < 0.05$ ,  $FC > 2.0$ ). Predicted upstream regulators of these genes were  
304 *HNF4A* (inhibited,  $p = 2.3E-04$ ) and  $IFN\gamma$  (activated,  $p = 5.2E-05$ ). At the colonic level, we identified 54  
305 differentially expressed genes in *ACE2* positive cells from inflamed colon, as compared to control tissue.

306 TNF, lipopolysaccharides, IFN $\gamma$  and IL-1 $\beta$  were predicted as top ranked upstream regulators (activated,  
307  $p \leq 1.9E-15$ )

308

309 **Inflammatory stimuli result in upregulation of *ACE2* and *TMPRSS2* in organoids from IBD**  
310 **patients but not from healthy individuals**

311 Because of the clear upregulation of *ACE2* in inflamed colonic mucosa (**Figure 1A**) and the prediction of  
312 TNF as key regulator in *ACE2* positive cells, we investigated the effect of an inflammatory stimulus on *ACE2*  
313 expression in an *ex vivo* organoid model. In organoids derived from controls, inflammatory stimuli did not  
314 affect *ACE2* expression ( $p=9.1E-01$ ) (**Figure 7A**). Strikingly, in organoids derived from inflamed or  
315 uninfamed colonic biopsies from UC patients, addition of an inflammatory stimulus did significantly  
316 upregulate *ACE2* (FC=2.4,  $p=1.7E-02$ ; FC=2.0,  $p=2.9E-02$ ) (**Figure 7A**). No significant effect on *DPP4*  
317 expression could be observed ( $p=7.4E-02$ ;  $p=7.9E-01$ ), whereas *TMPRSS2* was significantly upregulated  
318 after inflammatory stimulation (FC=2.6,  $p=5.1E-14$ ; FC=2.8,  $p=1.5E-30$ ) (**Figure 7B-C**).

319

320 **Anti-TNF therapy restores colonic, but not ileal, epithelial *ACE2* dysregulation in anti-TNF**  
321 **responders**

322 Given the *ex vivo* model clearly confirmed the effect of a pro-inflammatory mix, including TNF, on epithelial  
323 *ACE2* expression, we subsequently studied the effect of neutralizing TNF (through administration of  
324 infliximab) on intestinal *ACE2* expression in IBD patients with active endoscopic disease. Paired  
325 transcriptomic data, generated prior to first infliximab administration and 4-6 weeks after treatment initiation,  
326 confirmed a significant downregulation of colonic *ACE2* in endoscopic remitters, but not in non-remitters  
327 ( $p=1.8E-04$ ,  $p=6.5E-01$  respectively) (**Supplementary Figure S6**). In contrast, infliximab therapy did not  
328 significantly affect ileal *ACE2* expression in remitters and non-remitters ( $p=7.8E-02$ ,  $p=2.25E-01$   
329 respectively).

330

## 331 DISCUSSION

332 Many patients with IBD have long-term exposure to corticosteroids, thiopurines, methotrexate, small  
333 molecules and/or biological agents, classifying them as high-risk patients because of their  
334 immunosuppression. In addition, intestinal inflammation has shown to be an important risk factor for SARS-  
335 CoV-2 infection and prognosis in IBD.<sup>14, 15, 16, 17, 18</sup> However, emerging evidence now suggests that IBD  
336 patients do not seem more vulnerable for COVID-19. To reconcile these observations, we investigated the  
337 role of intestinal inflammation on the potential viral intestinal entry mechanisms through bulk and single cell  
338 transcriptomics, immunofluorescence and *ex vivo* organoid cultures in patients with IBD.

339  
340 In contrast to previous bulk data,<sup>40</sup> we observed significant alterations in intestinal *ACE2* expression  
341 depending on the location and inflammatory state, both at tissue and single cell mRNA level, as at protein  
342 level. *ACE2* expression was limited exclusively to epithelial cells, both in ileum and colon. Hence, *ACE2*  
343 dysregulation in bulk transcriptomics as a result of massive influx of immunocytes at the site of inflammation  
344 could be excluded.

345  
346 It is conceived that SARS-CoV-2 infects epithelial cells, causing cytokine and chemokine release, resulting  
347 in acute intestinal inflammation characterized by infiltration of neutrophils, macrophages and T cells,<sup>41</sup> with  
348 associated shedding of faecal calprotectin and increased systemic IL-6 response,<sup>42</sup> and IFN signaling.<sup>7</sup>  
349 Similar to recent data,<sup>43, 44, 45</sup> we found a significant downregulation of *ACE2* in inflamed ileum and a  
350 significant *ACE2* upregulation in inflamed colon. This opposing effect of inflammation on intestinal *ACE2*  
351 expression in small and large intestine was striking, which could be attributed - based on sc-RNA data - to  
352 different key transcription factors active between ileal and colonic *ACE2* positive cells.

353  
354 Being an IBD susceptibility locus,<sup>46</sup> epithelial HNF4A plays a protective role in IBD by consolidating the  
355 epithelial barrier,<sup>47</sup> especially in small intestine.<sup>48</sup> As it appears to be a transcriptional sensor of  
356 inflammation,<sup>49</sup> and because of its key role as transcription factor in the regulation of angiotensinogen  
357 metabolism,<sup>50</sup> the decrease in *ACE2* in inflamed ileum does therefore not come as a surprise. In individuals  
358 carrying the minor AA genotype at the IBD HNF4A susceptibility locus, ileal *ACE2* expression was even  
359 further downregulated, without any effect on colonic *ACE2*. Of note, our sc-RNAseq data showing *ACE2*

360 downregulation in enterocytes from inflamed CD ileum further suggest an intrinsic regulation of *ACE2*. In  
361 addition, as we observed significant correlations between enterocyte markers and ileal *ACE2* as well as an  
362 overall decrease in number of cells expressing *ACE2* in inflamed CD ileum, a loss of enterocytes might also  
363 explain lower *ACE2* levels.

364  
365 Remarkably, a very recent GWAS study identified 3p21.31 as a genetic locus being associated with COVID-  
366 19–induced respiratory failure.<sup>51</sup> This locus covers a cluster of 6 genes (*SLC6A20*, *LZTFL1*, *CCR9*, *FYCO1*,  
367 *CXCR6*, and *XCR1*), with the identified risk allele (i.e. worse COVID-19 outcome) being associated with  
368 increased *SCL6A20* expression. Strikingly, *SCL6A20* is known to be regulated by *HNF4A*.<sup>52</sup>

369  
370 Although the colonic *ACE2* co-expression cluster in bulk tissue was also enriched for *HNF4A* as upstream  
371 transcriptional regulator, single cell data revealed that colonic *ACE2* expression seems primarily driven by  
372 interferon regulator factors. Upstream regulating analysis further supported that pro-inflammatory  
373 cytokines, including TNF, IFN $\gamma$  and IL-1 $\beta$  contribute to colonic *ACE2* upregulation. Elevated colonic *ACE2*  
374 levels in patients with active inflammation may thus promote viral entry and, in theory, could promote  
375 COVID-19 disease severity. One can question this hypothesis as downregulated *ACE2* in inflamed ileum  
376 remains much higher than in normal and IBD colon. However, *ACE2* expression is the most abundant in  
377 the small intestine, followed by the large intestine, whereas its expression is limited in the respiratory  
378 system.<sup>53, 54</sup> While there is yet no direct evidence that altered expression of intestinal *ACE2* directly impacts  
379 SARS-CoV-2 intestinal entry and tropisms to different intestinal sites,<sup>55</sup> using *ex vivo* organoid models we  
380 confirmed that pro-inflammatory cytokines can upregulate colonic epithelial *ACE2* expression in IBD  
381 patients, but not in healthy individuals. Different genetic susceptibility and/or microbial composition may be  
382 responsible for difference in response to inflammatory stimuli observed in controls and IBD. Indeed, it has  
383 already been demonstrated that organoids from UC patients maintain some inherent differences as  
384 compared to non-IBD tissue,<sup>19, 56</sup> presumably reflecting inherent genetic factors which could result in a more  
385 sensitive epithelium.

386  
387 Being the key example of a complex immune-mediated entity where environmental and microbial factors  
388 modulate the immune response in a genetically susceptible host,<sup>57</sup> the differences in *ACE2* expression  
389 upon inflammatory stimuli between colon and ileum in patients with IBD may also be attributed to

390 differences in the intestinal microbiome. Lipopolysaccharides, comprising the wall of gram-negative  
391 bacteria, was indeed identified as one of the key drivers of the *ACE2* gene cluster in colon, but not in ileum.  
392 However, blind use of antibiotics or probiotics for COVID-19 is not recommended until a better  
393 understanding of the effect of SARS-CoV-2 on gut microbiota is obtained.<sup>58</sup>

394

395 In line with our findings, national and international registries suggest active IBD as a risk factor for  
396 (complicated) COVID-19.<sup>14, 15, 16, 17, 18</sup> Adequate disease management, by appropriate dampening of  
397 intestinal inflammation, therefore seems key in preventing IBD patients from COVID-19. Because of the  
398 significant *ACE2* upregulation in colon, one might consider that active UC patients and/or CD patients with  
399 colonic involvement could be at higher risk for (complicated) COVID-19, compared to ileal CD. Although  
400 international registries did not yet report any outcome data split by disease location, our data would suggest  
401 an increased risk for complicated COVID-19 depending on disease location and disease activity.

402

403 Of note, several key cytokines implicated in IBD pathogenesis,<sup>57, 59</sup> and also key drivers of *ACE2* colonic  
404 expression in this study, are currently under investigation as potential therapeutic targets for COVID-19,  
405 including TNF, IFN $\gamma$ , IL-1 $\beta$  and IL-6.<sup>60</sup> Although further evidence is warranted if these anti-cytokine  
406 therapies can dampen the observed cytokine storm in COVID-19, we demonstrated that anti-TNF therapy  
407 does restore intestinal *ACE2* dysregulation in a subset of IBD patients.

408

409 Although we acknowledge the lack of data on SARS-CoV-2 infected patients, a sequencing depth not  
410 enabling to look for *HNF4A* alternative splicing and isoforms with pro- and anti-inflammatory effects,<sup>61</sup> and  
411 the lack of additional functional validation experiments, the replication of our findings on several levels  
412 (tissue and single cell gene expression, protein expression and *ex vivo* models) highlights the impact of our  
413 observations for the management of IBD patients in the current COVID-19 crisis. Current guidelines do not  
414 promote stopping of immunosuppressive and biological drugs in IBD patients without symptoms suggestive  
415 of COVID-19. On the contrary, immunosuppressive and biological drugs may protect against the  
416 development of severe forms of COVID-19 infection.<sup>62</sup>

417

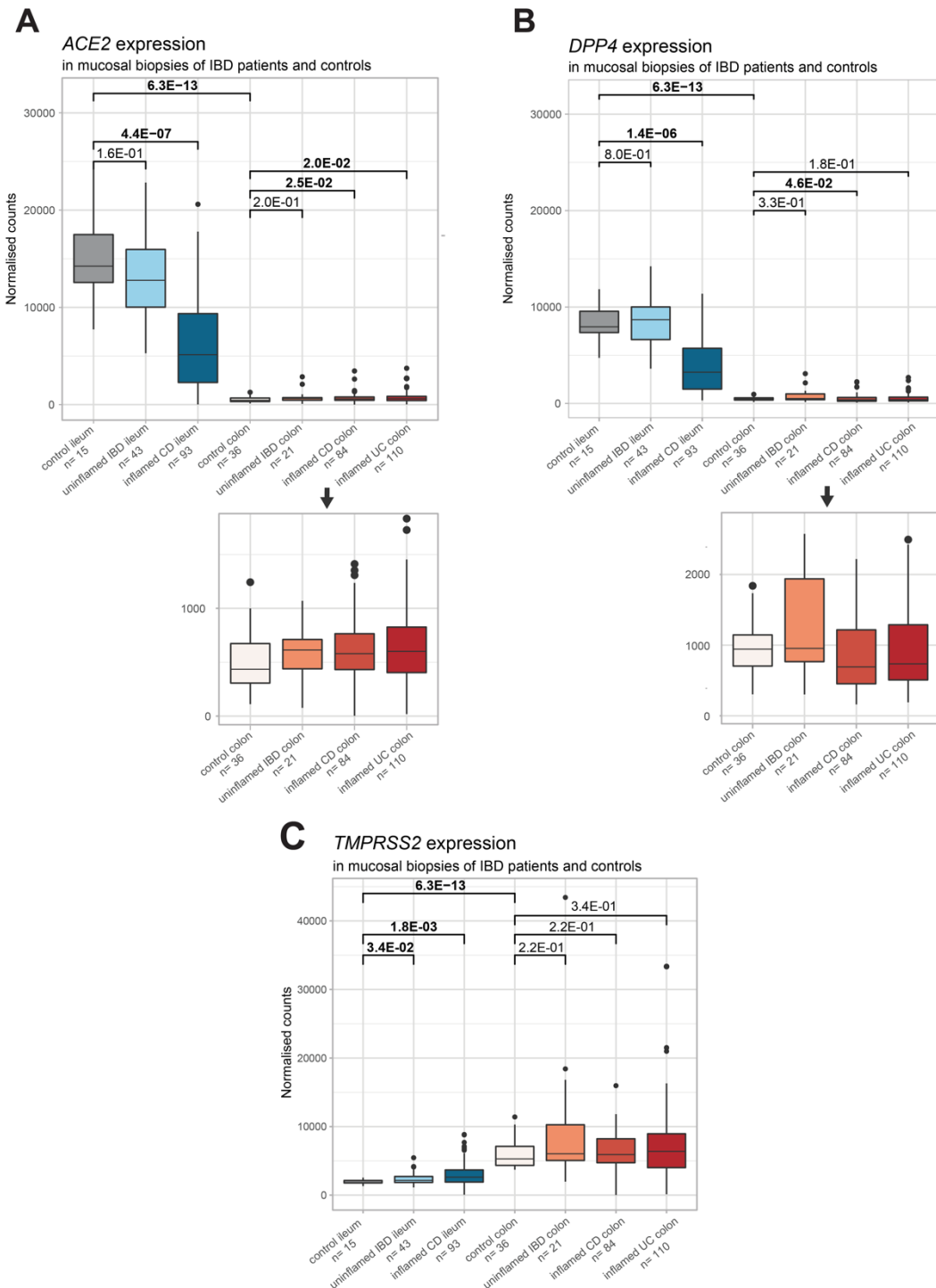
418 In conclusion, using bulk and single cell transcriptomic datasets, as well as *ex vivo* organoid cultures, we  
419 demonstrated that intestinal inflammation could alter SARS-CoV-2 entry mechanisms in the intestinal



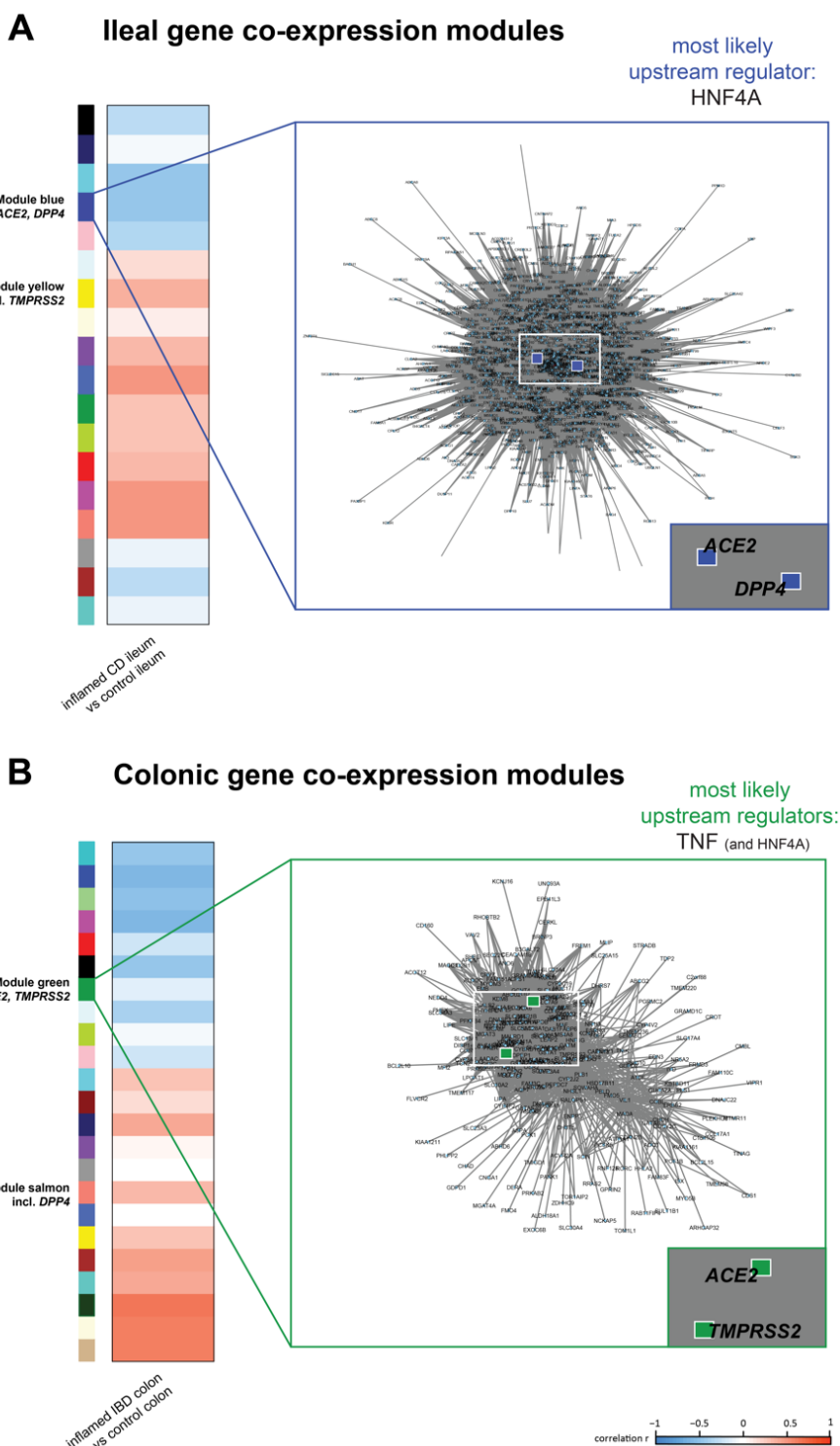
420 epithelium, with opposing effects seen in ileum and colon. *HNF4A*, an IBD susceptibility gene and  
421 transcriptional regulator of one of the key Covid-19 GWAS loci, is an important upstream regulator of *ACE2*  
422 expression in ileal tissue. In contrast, colonic *ACE2* expression depends on interferon regulating factors  
423 and pro-inflammatory cytokines. Overall, our translational data provide further evidence for the clinical  
424 recommendation to pursue adequate disease control in patients with IBD to reduce the risk of (complicated)  
425 COVID-19.  
426

427 **FIGURES**

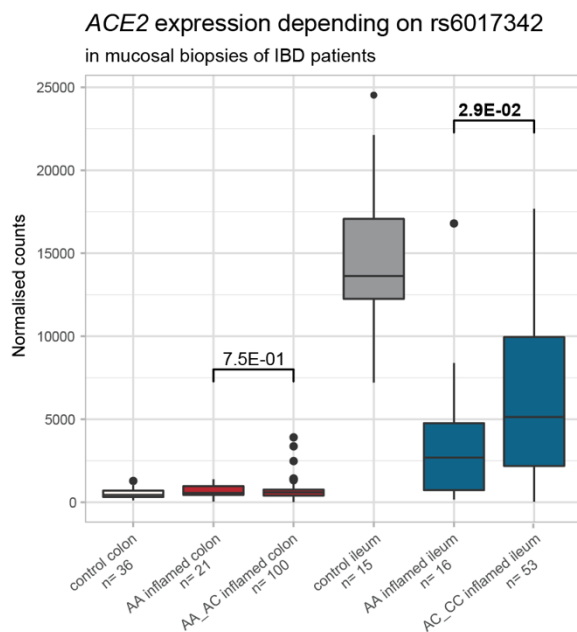
428 **Figure 1: Mucosal ACE2, DPP4 and TMPRSS2 in IBD patients and controls.** (A) Boxplots of mucosal ACE2 as measured by RNA  
 429 sequencing (normalized counts). (B) Boxplots of mucosal DPP4 as measured by RNA sequencing (normalized counts). (C) Boxplots  
 430 of mucosal TMPRSS2 as measured by RNA sequencing (normalized counts). Significant comparisons are highlighted in bold.  
 431 CD, Crohn's disease; control, non-IBD controls; IBD, inflammatory bowel disease; UC, ulcerative colitis  
 432



433 **Figure 2: Gene co-expression**  
 434 **analysis of the ACE2-, DPP4-**  
 435 **and TMPRSS2-related**  
 436 **networks.** WGCNA was applied  
 437 on mucosal biopsies of **(A)** IBD  
 438 ileum and non-IBD control ileum,  
 439 and **(B)** IBD colon and non-IBD  
 440 control colon. A positive  
 441 correlation (highlighted in red)  
 442 means an upregulation in  
 443 disease as compared to matched  
 444 controls, while a negative  
 445 correlation (highlighted in blue)  
 446 refers to a downregulation in  
 447 disease. The reported networks  
 448 visualize genes having a  
 449 correlation value of  $\geq 0.85$  with  
 450 the module eigengene.  
 451 CD, Crohn's disease; control, non-IBD  
 452 controls; IBD, inflammatory bowel disease;  
 453 incl., including; WGCNA, Weighted Gene  
 454 Co-expression Network Analysis;  
 455  
 456

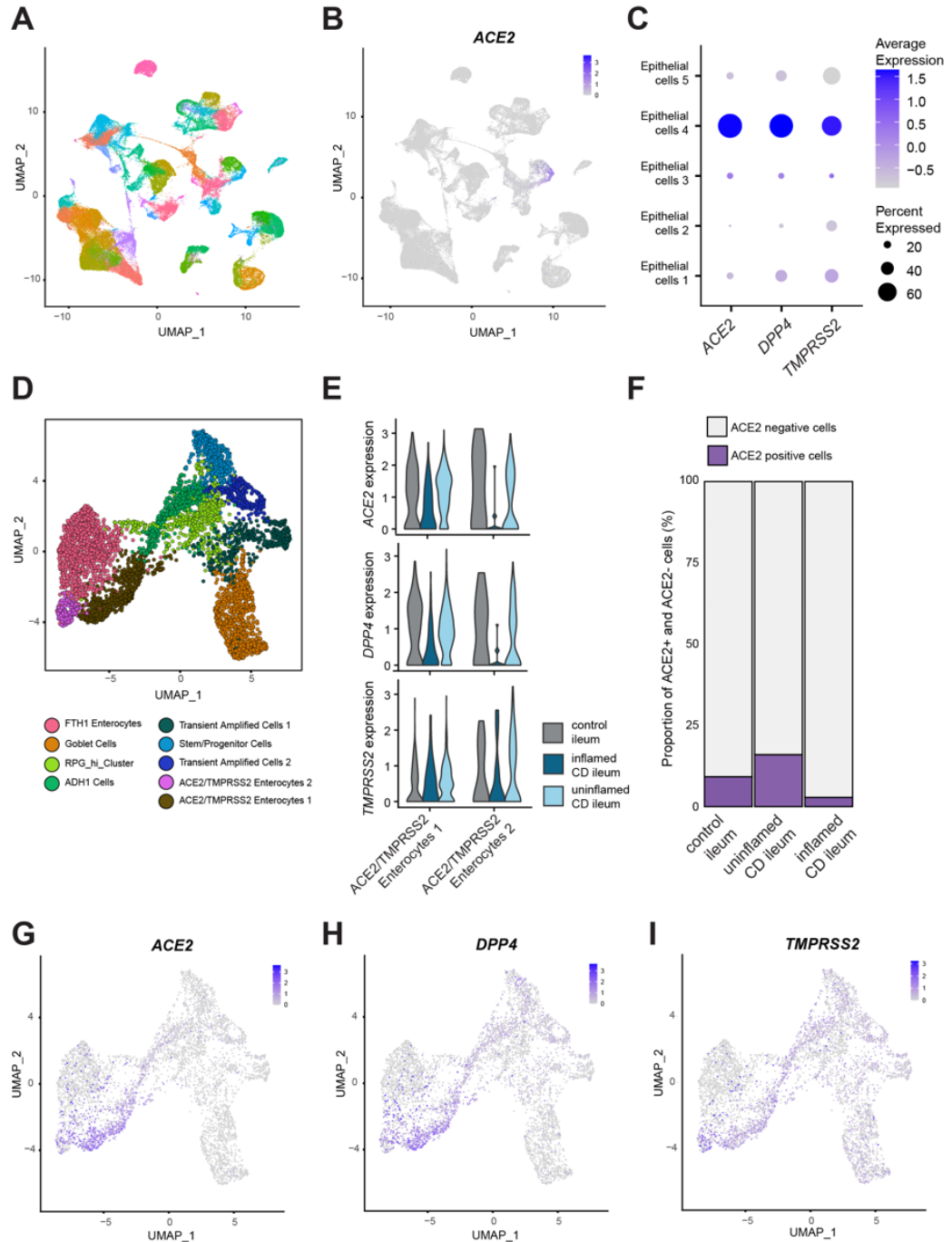


457 **Figure 3: Mucosal *ACE2* and *HNF4A* in IBD patients and controls depending on rs6017342 genotype.** Boxplots of mucosal  
458 *ACE2* as measured by RNA sequencing (normalized counts). Significant comparisons are highlighted in bold.  
459 controls, non-IBD controls  
460  
461



462 **Figure 4: Decrease of ACE2/TMPRSS2 double positive cells in inflamed ileum in CD patients.** (A) Uniform Manifold Approximation and Projection (UMAP) plot showing  
 463 unsupervised clustering of integrated single cell RNA sequencing data from control, uninfamed and inflamed ileal tissue. (B) Expression of *ACE2* overlaid on the UMAP plot as  
 464 in A. (C) Expression of *ACE2*, *DPP4*, and *TMPRSS2* in ileal epithelial cells. (D) UMAP showing epithelial sub clusters obtained upon re-clustering only the epithelial cells in ileum.  
 465 (E) Expression and distribution of *ACE2*, *DPP4*, and *TMPRSS2* in the two enterocyte clusters co expressing *ACE2* and *TMPRSS2* split between control, uninfamed and inflamed  
 466 samples. (F) Proportion of ACE2+ and ACE2- cells in control, uninfamed and inflamed samples in the ileal epithelial cells. (G-I) Gene expression overlaid on the UMAP Plot as  
 467 in panel D of *ACE2*, *DPP4* and *TMPRSS2* respectively.  
 468 CD, Crohn's disease; control, non-IBD controls

470



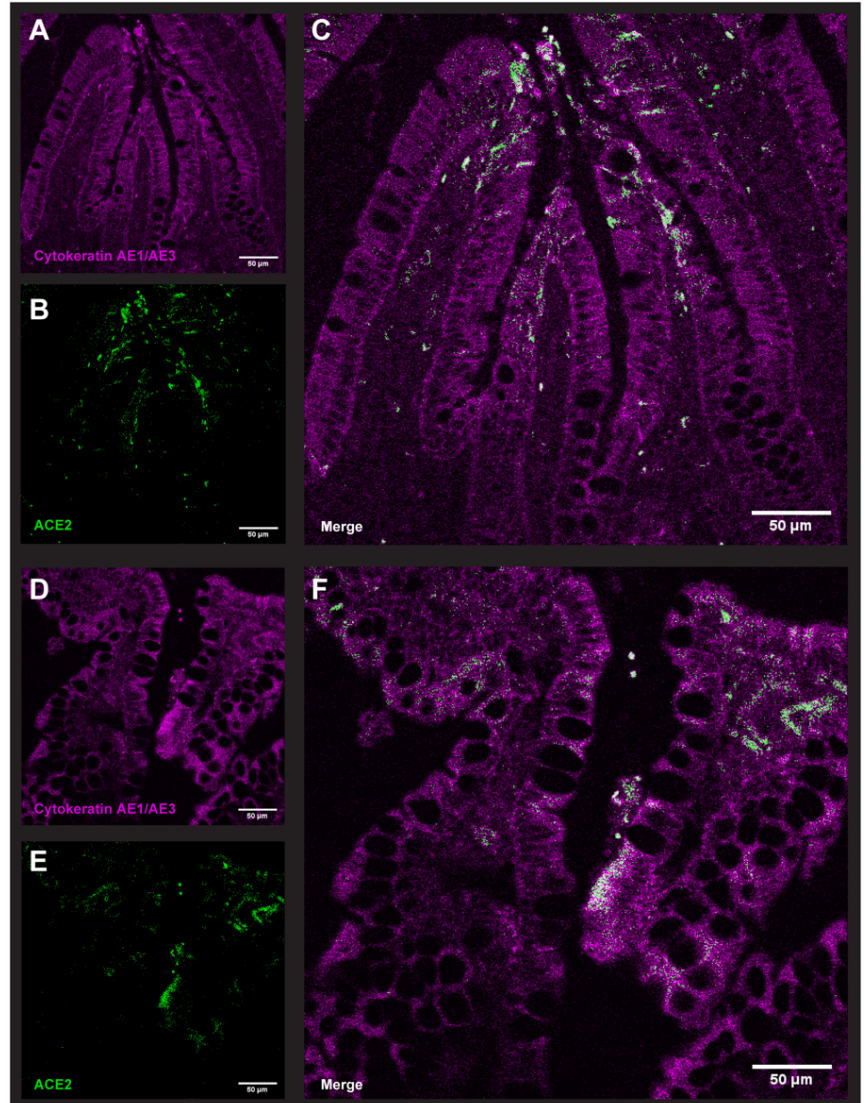
471 **Figure 5: Cytokeratin AE1/AE3 and ACE2 expression in human gut.**

472 Confocal microscopy images of human gut in which ACE2 positive epithelial cells were stained with cytokeratin AE1/AE3 (magenta)

473 and ACE2 (green). The scale bar in the immunofluorescent image represents 50  $\mu$ m. Normal ileum from patient with colorectal cancer

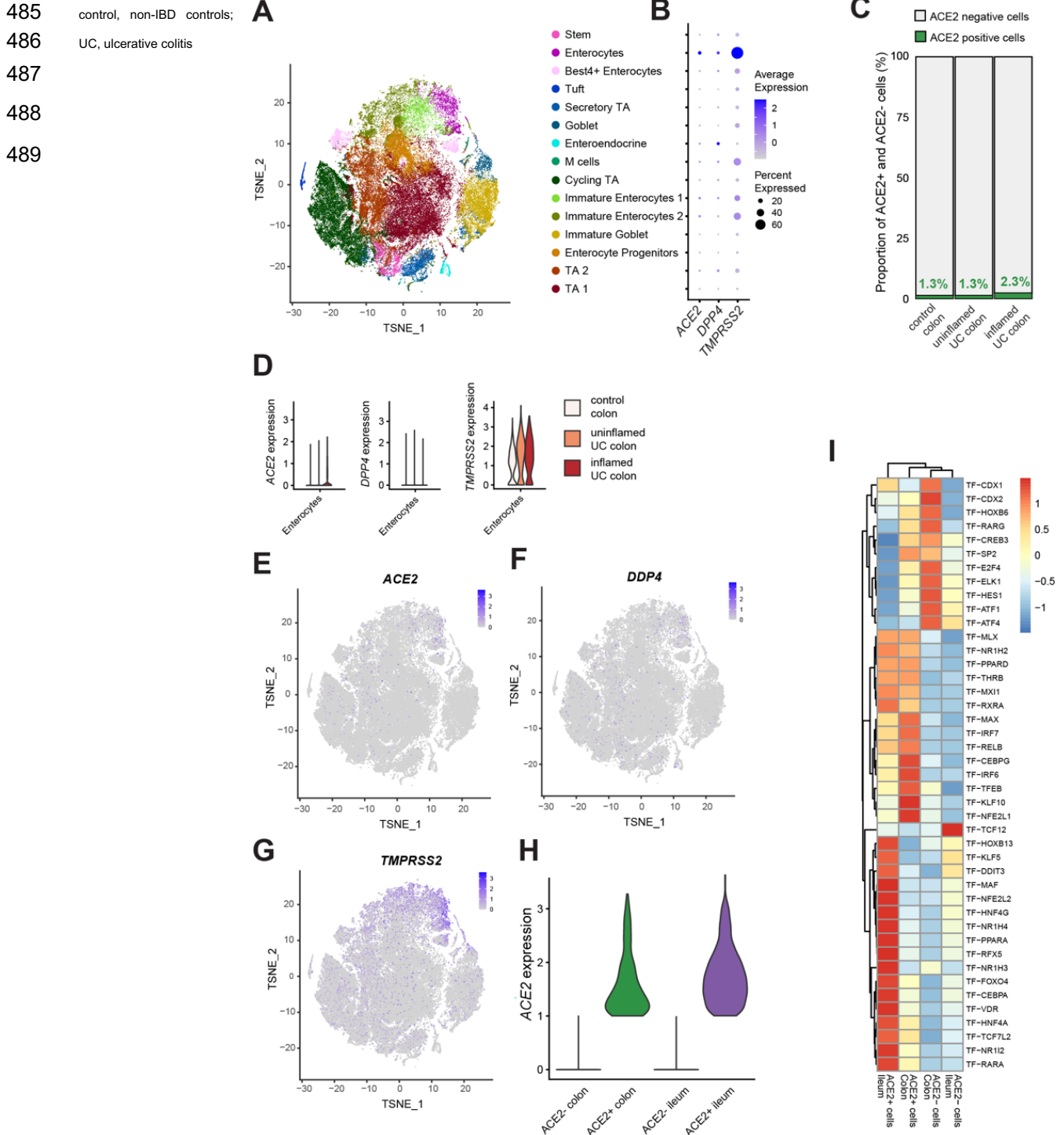
474 (A-C); inflamed ileum from patient with Crohn's disease (D-F).

475



476

477 **Figure 6: Increase colonic *ACE2* expression in the epithelial cells of patient with active UC.** (A) t-distributed stochastic neighbor  
 478 embedding (tSNE) plot showing the clustering and annotation of epithelial cells from the colon as reported in Smillie et al.<sup>31</sup> (B)  
 479 Expression of *ACE2*, *DPP4* and *TMPRSS2* in epithelial cell clusters of the colon. (C) Proportion of *ACE2*+ colonic epithelial cells in  
 480 control, uninfamed and inflamed samples. (D) Expression of *ACE2*, *DPP4* and *TMPRSS2* in colonic enterocytes for control,  
 481 uninfamed and inflamed samples. (E-G) Expression of *ACE2*, *DPP4*, and *TMPRSS2* overlaid on tSNE shown in panel A. (H)  
 482 Expression level of *ACE2* in *ACE2*+ cells of colon and ileum. (I) Heatmap showing scaled area under the curve (AUC) values of top  
 483 15 specific and highly enriched regulons (average AUC >0.1) in *ACE2*+ or *ACE2*- compartments in integrated data of ileal and colonic  
 484 single cell data identified by SCENIC analysis.



490 **Figure 7: Organoid *ACE2*, *DPP4* and *TMPRSS2* in UC patients and controls with and without addition of an inflammatory mix.**

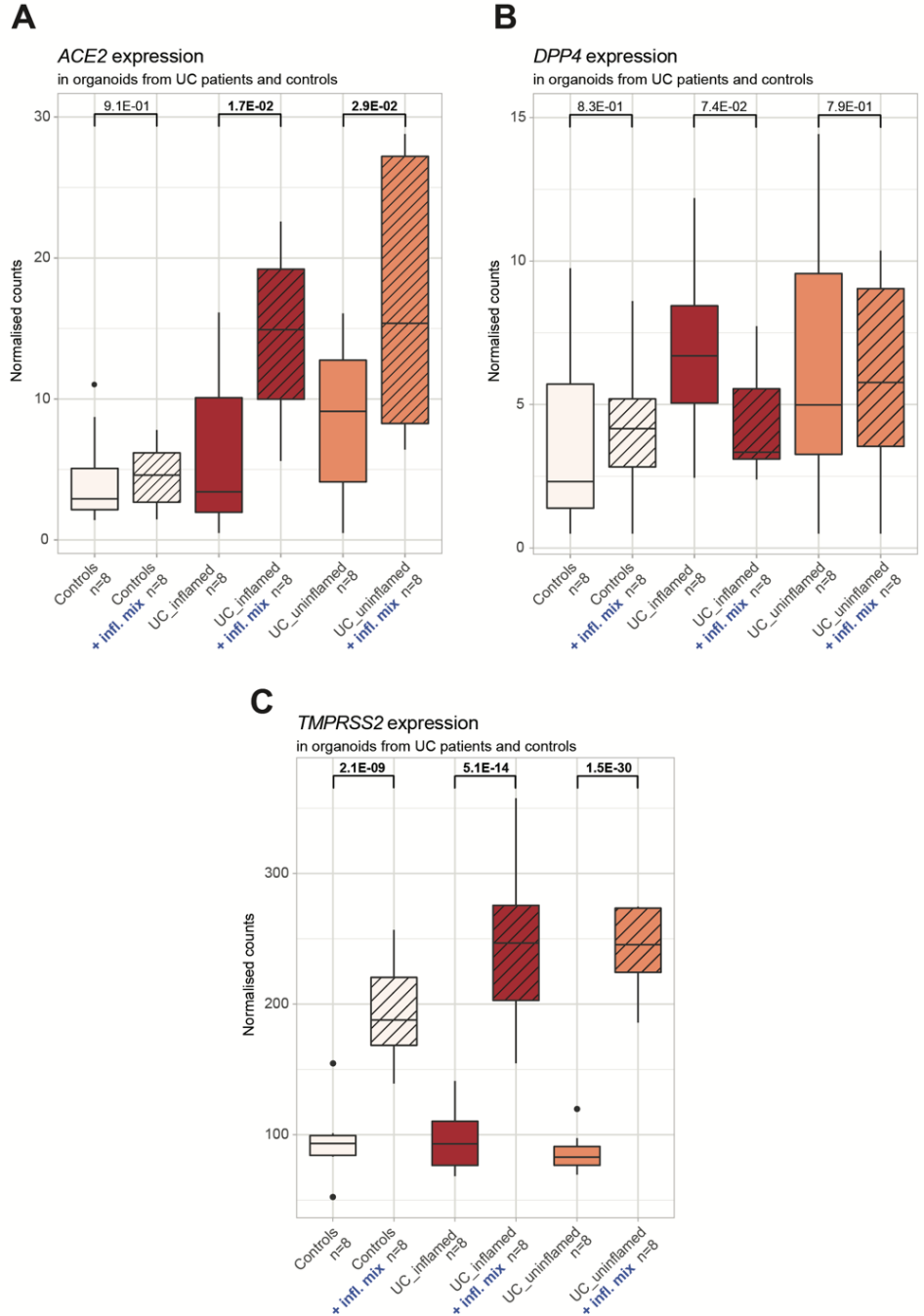
491 **(A)** Boxplots of organoid *ACE2* as measured by RNA sequencing (normalized counts). **(B)** Boxplots of organoid *DPP4* as measured

492 by RNA sequencing (normalized counts). **(C)** Boxplots of organoid *TMPRSS2* as measured by RNA sequencing (normalized counts).

493 Significant comparisons are highlighted in bold.

494 control, non-IBD controls; IBD, inflammatory bowel disease; UC, ulcerative colitis

495



496



## 497 SUPPLEMENTARY FIGURES

498 **Supplementary Figure 1: Correlation between mucosal *ACE2* levels and mucosal *HNF4A* levels in**  
499 **patients with IBD and controls.** Correlation between normalized *ACE2* counts and normalized *HNF4A*  
500 counts in ileal (A) and colonic (B) tissue from IBD patients and controls

501  
502 **Supplementary Figure 2: Correlation between ileal *ACE2* levels and ileal epithelial marker gene**  
503 **levels in patients with IBD and controls.** Correlation between normalized ileal *ACE2* counts and  
504 normalized epithelial marker gene counts: *APOA1* (A), *SI* (B), *FABP6* (C) and *ENPEP* (D)

505  
506 **Supplementary Figure 3: Ileal epithelial cell subtypes annotation and sub clusters expression of**  
507 ***ACE2*, *DPP4* and *TMPRSS2*.** (A) Heatmap showing the SingleR score for annotation of the 61 cell clusters  
508 of the ileum dataset. (B) Barplot showing the distribution of control, uninfamed and inflamed sample types  
509 in the 78,722 cells sequenced from ileum. (C) Expression of various epithelial sub type markers in the  
510 epithelial sub clusters of the ileum. (D) Expression of *ACE2*, *DPP4* and *TMPRSS2* in the epithelial sub  
511 clusters. E) Expression of *ACE2*, *DPP4* and *TMPRSS2* in the epithelial sub clusters split between control,  
512 uninfamed and inflamed sample type.

513  
514 **Supplementary Figure 4: Colonic epithelial cell subtypes annotation and sub clusters expression**  
515 **of *ACE2*, *DPP4* and *TMPRSS2*.** (A-C) Expression of *ACE2* in the colonic epithelial cells, immune cells and  
516 stromal cells. D) Expression of epithelial subtype markers in colonic epithelial clusters. (D) Expression of  
517 *ACE2*, *DPP4* and *TMPRSS2* in colonic epithelial clusters split between sample types of control, uninfamed  
518 and inflamed sample type.

519  
520 **Supplementary Figure 5: Integrated analysis of epithelial cells from colon and ileum.** (A) Proportion  
521 of *ACE2*+ cells in epithelial clusters of ileum and colon from the integrated analysis of single cell data of  
522 colon and ileum. (B) Contribution of the subclusters of colonic and ileal epithelial cells to *ACE2*+ and *ACE2*-  
523 compartments in colon and ileum.

524

525 **Supplementary Figure 6: Colonic *ACE2* expression in IBD patients prior and after anti-TNF therapy.**

526 Boxplots of normalized log<sub>2</sub> transformed *ACE2* expression levels prior to and 4-6 weeks after infliximab  
527 therapy in colonic mucosa of IBD patients, split by endoscopic remission.

528 Endoscopic remission in UC : Mayo endoscopic sub-score 0-1; endoscopic remission in CD : complete absence of ulcerations

529

530 **TABLES**

531 **Supplementary Table 1: Demographics of all included patients**

532 **Supplementary Table 2: Genes within ileal *ACE2*-coexpression module**

533 **Supplementary Table 3: Genes within colonic *ACE2*-coexpression module**

534

535

## 536 REFERENCES

- 537 1. World Health Organization. Coronavirus disease (COVID-2019) situation reports.) (2020).  
538
- 539 2. Huang C, *et al.* Clinical features of patients infected with 2019 novel coronavirus in Wuhan,  
540 China. *Lancet* **395**, 497-506 (2020).  
541
- 542 3. Xiao F, Tang M, Zheng X, Liu Y, Li X, Shan H. Evidence for Gastrointestinal Infection of SARS-  
543 CoV-2. *Gastroenterology* **158**, 1831-1833 e1833 (2020).  
544
- 545 4. Mao R, *et al.* Manifestations and prognosis of gastrointestinal and liver involvement in patients  
546 with COVID-19: a systematic review and meta-analysis. *Lancet Gastroenterol Hepatol*, (2020).  
547
- 548 5. Lamers MM, *et al.* SARS-CoV-2 productively infects human gut enterocytes. *Science*, (2020).  
549
- 550 6. Sungnak W, *et al.* SARS-CoV-2 entry factors are highly expressed in nasal epithelial cells  
551 together with innate immune genes. *Nat Med*, (2020).  
552
- 553 7. Ziegler C, *et al.* SARS-CoV-2 receptor ACE2 is an interferon-stimulated gene in human airway  
554 epithelial cells and is detected in specific cell subsets across tissues.  
555
- 556 8. Hoffmann M, *et al.* SARS-CoV-2 Cell Entry Depends on ACE2 and TMPRSS2 and Is Blocked by  
557 a Clinically Proven Protease Inhibitor. *Cell* **181**, 271-280 e278 (2020).  
558
- 559 9. Li Y, *et al.* The MERS-CoV receptor DPP4 as a candidate binding target of the SARS-CoV-2  
560 spike. *iScience*, 101160 (2020).  
561
- 562 10. Zhou J, *et al.* Human intestinal tract serves as an alternative infection route for Middle East  
563 respiratory syndrome coronavirus. *Sci Adv* **3**, eaao4966 (2017).  
564
- 565 11. van de Veerdonk FL, *et al.* A systems approach to inflammation identifies therapeutic targets in  
566 SARS-CoV-2 infection. *medRxiv*, 2020.2005.2023.20110916 (2020).  
567
- 568 12. Singer D, *et al.* Defective intestinal amino acid absorption in Ace2 null mice. *Am J Physiol*  
569 *Gastrointest Liver Physiol* **303**, G686-695 (2012).  
570
- 571 13. Hashimoto T, *et al.* ACE2 links amino acid malnutrition to microbial ecology and intestinal  
572 inflammation. *Nature* **487**, 477-481 (2012).  
573
- 574 14. Bezzio C, *et al.* Outcomes of COVID-19 in 79 patients with IBD in Italy: an IG-IBD study. *Gut*,  
575 (2020).  
576
- 577 15. Brenner E, Ungaro R, Colombel J, Kappelman M. SECURE-IBD Database Public Data Update.)  
578 (2020).  
579
- 580 16. Taxonera C, Sagastagoitia I, Alba C, Mañas N, Olivares D, Rey E. 2019 Novel Coronavirus  
581 Disease (COVID-19) in patients with Inflammatory Bowel Diseases. *Alimentary Pharmacology &*  
582 *Therapeutics n/a*.  
583
- 584 17. Lukin DJ, Kumar A, Hajifathalian K, Sharaiha RZ, Scherl EJ, Longman RS. Baseline Disease  
585 Activity and Steroid Therapy Stratify Risk of COVID-19 in Patients with Inflammatory Bowel  
586 Disease. *Gastroenterology*.  
587
- 588 18. Khan N, Patel D, Xie D, Lewis J, Trivedi C, Yang Y-X. Impact of Anti-TNF and Thiopurines  
589 medications on the development of COVID-19 in patients with inflammatory bowel disease: A  
590 Nationwide VA cohort study. *Gastroenterology*.  
591

- 592 19. Arnauts K, Verstockt B, Santo Ramalho A, Vermeire S, Verfaillie C, Ferrante M. Ex vivo  
593 mimicking of inflammation in organoids derived from patients with ulcerative colitis.  
594 *Gastroenterology*, (2020).  
595
- 596 20. Verstockt B, *et al.* Expression Levels of 4 Genes in Colon Tissue Might Be Used to Predict Which  
597 Patients Will Enter Endoscopic Remission After Vedolizumab Therapy for Inflammatory Bowel  
598 Diseases. *Clin Gastroenterol Hepatol*, (2019).  
599
- 600 21. Kim D, Langmead B, Salzberg SL. HISAT: a fast spliced aligner with low memory requirements.  
601 *Nat Methods* **12**, 357-360 (2015).  
602
- 603 22. Anders S, Pyl PT, Huber W. HTSeq--a Python framework to work with high-throughput  
604 sequencing data. *Bioinformatics* **31**, 166-169 (2015).  
605
- 606 23. Yates A, *et al.* Ensembl 2016. *Nucleic Acids Res* **44**, D710-716 (2016).  
607
- 608 24. Love MI, Huber W, Anders S. Moderated estimation of fold change and dispersion for RNA-seq  
609 data with DESeq2. *Genome Biol* **15**, 550 (2014).  
610
- 611 25. Langfelder P, Horvath S. WGCNA: an R package for weighted correlation network analysis. *BMC*  
612 *Bioinformatics* **9**, 559 (2008).  
613
- 614 26. Verstockt B, *et al.* Mucosal IL13RA2 expression predicts nonresponse to anti-TNF therapy in  
615 Crohn's disease. *Aliment Pharmacol Ther*, (2019).  
616
- 617 27. Verstockt S, *et al.* Gene and Mirna Regulatory Networks During Different Stages of Crohn's  
618 Disease. *J Crohns Colitis*, (2019).  
619
- 620 28. Shannon P, *et al.* Cytoscape: a software environment for integrated models of biomolecular  
621 interaction networks. *Genome Res* **13**, 2498-2504 (2003).  
622
- 623 29. Arijis I, *et al.* Mucosal gene signatures to predict response to infliximab in patients with ulcerative  
624 colitis. *Gut* **58**, 1612-1619 (2009).  
625
- 626 30. Arijis I, *et al.* Predictive value of epithelial gene expression profiles for response to infliximab in  
627 Crohn's disease. *Inflamm Bowel Dis* **16**, 2090-2098 (2010).  
628
- 629 31. Smillie CS, *et al.* Intra- and Inter-cellular Rewiring of the Human Colon during Ulcerative Colitis.  
630 *Cell* **178**, 714-730 e722 (2019).  
631
- 632 32. Butler A, Hoffman P, Smibert P, Papalexi E, Satija R. Integrating single-cell transcriptomic data  
633 across different conditions, technologies, and species. *Nat Biotechnol* **36**, 411-420 (2018).  
634
- 635 33. Stuart T, *et al.* Comprehensive Integration of Single-Cell Data. *Cell* **177**, 1888-1902 e1821  
636 (2019).  
637
- 638 34. Aibar S, *et al.* SCENIC: single-cell regulatory network inference and clustering. *Nat Methods* **14**,  
639 1083-1086 (2017).  
640
- 641 35. Purcell S, *et al.* PLINK: a tool set for whole-genome association and population-based linkage  
642 analyses. *Am J Hum Genet* **81**, 559-575 (2007).  
643
- 644 36. Huang H, *et al.* Fine-mapping inflammatory bowel disease loci to single-variant resolution. *Nature*  
645 **547**, 173-178 (2017).  
646
- 647 37. Barker H, Parkkila S. Bioinformatic characterization of angiotensin-converting enzyme 2, the entry  
648 receptor for SARS-CoV-2. (2020).  
649

- 650 38. Aran D, *et al.* Reference-based analysis of lung single-cell sequencing reveals a transitional  
651 profibrotic macrophage. *Nat Immunol* **20**, 163-172 (2019).  
652
- 653 39. Wang Y, *et al.* Single-cell transcriptome analysis reveals differential nutrient absorption functions  
654 in human intestine. *J Exp Med* **217**, (2020).  
655
- 656 40. Burgueno JF, *et al.* Expression of SARS-CoV-2 Entry Molecules ACE2 and TMPRSS2 in the Gut  
657 of Patients With IBD. *Inflamm Bowel Dis* **26**, 797-808 (2020).  
658
- 659 41. Vabret N, *et al.* Immunology of COVID-19: current state of the science. *Immunity*, (2020).  
660
- 661 42. Effenberger M, *et al.* Faecal calprotectin indicates intestinal inflammation in COVID-19. *Gut*,  
662 (2020).  
663
- 664 43. Potdar AA, *et al.* Reduced expression of COVID-19 host receptor, *ACE2* is  
665 associated with small bowel inflammation, more severe disease, and response to anti-TNF  
666 therapy in Crohn's disease. *medRxiv*, (2020).  
667
- 668 44. Krzysztof NJ, Christoffer LJ, Rahul K, Ricanek P, Jonas H, Jack S. Age, inflammation and  
669 disease location are critical determinants of intestinal expression of SARS-CoV-2 receptor ACE2  
670 and TMPRSS2 in inflammatory bowel disease. *Gastroenterology*, (2020).  
671
- 672 45. Suárez-Fariñas M, *et al.* Intestinal inflammation modulates the expression of ACE2 and  
673 TMPRSS2 and potentially overlaps with the pathogenesis of SARS-CoV-2 related disease.  
674 *bioRxiv*, (2020).  
675
- 676 46. Umicevic Mirkov M, Verstockt B, Cleynen I. Genetics of inflammatory bowel disease: beyond  
677 NOD2. *Lancet Gastroenterol Hepatol* **2**, 224-234 (2017).  
678
- 679 47. Ahn SH, *et al.* Hepatocyte nuclear factor 4alpha in the intestinal epithelial cells protects against  
680 inflammatory bowel disease. *Inflamm Bowel Dis* **14**, 908-920 (2008).  
681
- 682 48. Montenegro-Miranda PS, *et al.* A Novel Organoid Model of Damage and Repair Identifies  
683 HNF4alpha as a Critical Regulator of Intestinal Epithelial Regeneration. *Cell Mol Gastroenterol*  
684 *Hepatol*, (2020).  
685
- 686 49. Babeu JP, Boudreau F. Hepatocyte nuclear factor 4-alpha involvement in liver and intestinal  
687 inflammatory networks. *World J Gastroenterol* **20**, 22-30 (2014).  
688
- 689 50. Yanai K, *et al.* Regulated expression of human angiotensinogen gene by hepatocyte nuclear  
690 factor 4 and chicken ovalbumin upstream promoter-transcription factor. *J Biol Chem* **274**, 34605-  
691 34612 (1999).  
692
- 693 51. Ellinghaus D, *et al.* Genomewide Association Study of Severe Covid-19 with Respiratory Failure.  
694 *N Engl J Med*, (2020).  
695
- 696 52. Fishilevich S, *et al.* GeneHancer: genome-wide integration of enhancers and target genes in  
697 GeneCards. *Database (Oxford)* **2017**, (2017).  
698
- 699 53. Uhlen M, *et al.* Proteomics. Tissue-based map of the human proteome. *Science* **347**, 1260419  
700 (2015).  
701
- 702 54. Hikmet F, Méar L, Uhlén M, Lindskog C. The protein expression profile of ACE2 in human  
703 tissues. *bioRxiv*, (2020).  
704
- 705 55. Neurath MF. Covid-19 and immunomodulation in IBD. *Gut*, (2020).  
706
- 707 56. Dotti I, *et al.* Alterations in the epithelial stem cell compartment could contribute to permanent  
708 changes in the mucosa of patients with ulcerative colitis. *Gut* **66**, 2069-2079 (2017).

- 709  
710 57. de Souza HS, Fiocchi C. Immunopathogenesis of IBD: current state of the art. *Nat Rev*  
711 *Gastroenterol Hepatol* **13**, 13-27 (2016).  
712  
713 58. Mak JWY, Chan FKL, Ng SC. Probiotics and COVID-19: one size does not fit all. *Lancet*  
714 *Gastroenterol Hepatol*, (2020).  
715  
716 59. Friedrich M, Pohin M, Powrie F. Cytokine Networks in the Pathophysiology of Inflammatory Bowel  
717 Disease. *Immunity* **50**, 992-1006 (2019).  
718  
719 60. Merad M, Martin JC. Pathological inflammation in patients with COVID-19: a key role for  
720 monocytes and macrophages. *Nat Rev Immunol*, (2020).  
721  
722 61. Chellappa K, *et al.* Opposing roles of nuclear receptor HNF4alpha isoforms in colitis and colitis-  
723 associated colon cancer. *Elife* **5**, (2016).  
724  
725 62. D'Amico F, Danese S, Peyrin-Biroulet L, taskforce EC. Inflammatory bowel disease management  
726 during the COVID-19 outbreak: a survey from the European Crohn's and Colitis Organization  
727 (ECCO). *Gastroenterology*, (2020).  
728  
729  
730  
731

## 732 **ACKNOWLEDGEMENTS**

733 The authors would like to thank Vera Ballet, Helene Blevi, Sophie Organe, Nooshin Ardeshir Davani and Tamara Coopmans for an  
734 excellent job in maintaining the Biobank database; André D'Hoore and Gabriele Bislenghi (Department of Abdominal Surgery,  
735 University Hospitals Leuven, Belgium) for the resection specimens; Gabriele Dragoni and Brecht Creyns (Translational Research in  
736 GI disorders KU Leuven, Belgium) and Gert De Hertogh (Laboratory of Morphology and Molecular Pathology, University Hospitals  
737 Leuven, KU Leuven, Leuven, Belgium) for the processing of the resection specimens; Birgit Weynand, Lukas Marcelis and Matthias  
738 Van Haele (Laboratory of Morphology and Molecular Pathology, University Hospitals Leuven, KU Leuven, Leuven, Belgium) for the  
739 ACE2 antibody; David Carbonez, Kristine Stepnayan, Nina Dedoncker, Vanessa Brys, Jens Van Bouwel, Wim Meert, Alvaro Cortes  
740 Calabuig and Wouter Bossuyt (Genomics Core Facility, University Hospitals Leuven, Belgium) for the technical assistance with the  
741 RNA-sequencing library preparation and sequencing. Immunostainings were recorded on a Zeiss LSM 780 – SP Mai Tai HP DS (Cell  
742 and Tissue Imaging Cluster (CIC), supported by Hercules AKUL/11/37 and FWO G.0929.15 to Pieter Vanden Berghe, KU Leuven,  
743 Leuven, Belgium.

## 744 **AUTHOR CONTRIBUTIONS**

745 BV and SV contributed equally and share the first authorship. GM and SV contributed equally and shared the senior authorship.  
746 BV: study design, data acquisition and interpretation, statistical analysis and drafting of the manuscript. SaV: study design, data  
747 acquisition and interpretation, statistical analysis and drafting of the manuscript. SAR: data acquisition and interpretation (single cell  
748 RNA), statistical analysis and critical revision of the manuscript. BJK: data acquisition and interpretation (single cell RNA and  
749 immunostainings) and critical revision of the manuscript. KA: data acquisition and interpretation (organoid data), statistical analysis  
750 and critical revision of the manuscript. IC: data acquisition (genetics) and critical revision of the manuscript. JS: data interpretation  
751 and critical revision of the manuscript. MF: data interpretation and critical revision of the manuscript. GM: supervision, data acquisition  
752 and interpretation, critical revision of the manuscript. SV: study design, supervision, data interpretation and critical revision of the  
753 manuscript. All authors agreed on the final manuscript.  
754 Guarantor of the manuscript: Séverine Vermeire.

## 755 **CONFLICTS OF INTEREST**

756 B Verstockt reports financial support for research from Pfizer; lecture fees from Abbvie, Ferring, Takeda Pharmaceuticals, Janssen  
757 and R Biopharm; consultancy fees from Janssen and Sandoz.  
758 J Sabino reports lecture fees from Abbvie, Takeda, Janssen and Nestle Health Sciences.  
759 M Ferrante reports financial support for research: Amgen, Biogen, Janssen, Pfizer, Takeda, Consultancy: Abbvie, Boehringer-  
760 Ingelheim, MSD, Pfizer, Sandoz, Takeda and Thermo Fisher; Speakers fee: Abbvie, Amgen, Biogen, Boehringer-Ingelheim, Falk,  
761 Ferring, Janssen, Lamepro, MSD, Mylan, Pfizer, Sandoz, and Takeda.  
762 G Matteoli received financial support for research from DSM Nutritional Products, Karyopharm Therapeutics and Janssen.  
763 S Vermeire reports financial support for research: MSD, AbbVie, Takeda, Pfizer, J&J; Lecture fee(s): MSD, AbbVie, Takeda, Ferring,  
764 Centocor, Hospira, Pfizer, J&J, Genentech/Roche; Consultancy: MSD, AbbVie, Takeda, Ferring, Centocor, Hospira, Pfizer, J&J,  
765 Genentech/Roche, Celgene, Mundipharma, Celltrion, SecondGenome, Prometheus, Shire, Prodigest, Gilead, Galapagos.



766 S Verstockt, S Abdu Rahiman, BJ Ke, K Arnouts and I Cleynen declare no conflicts of interest.

## 767 **FUNDING**

768 K Arnouts is a doctoral fellow and S Vermeire and M Ferrante are Senior Clinical Investigators of the Research Foundation Flanders  
769 (FWO), Belgium. G Matteoli laboratory is supported by a FWO grant (G.0D83.17N), a grant from the International Organization for the  
770 Study of Inflammatory Bowel Diseases (IOIBD), a grant from the European Crohn's and Colitis Organization (ECCO) and grants from  
771 the KU Leuven Internal Funds (C12/15/016 and C14/17/097). S Vermeire and G Matteoli are funded by Strategic Basic Research  
772 FWO grant (S008419N).

773

774